THE EIGENFUNCTION EXPANSION NODAL METHODS FOR THE EVEN-PARITY TRANSPORT EQUATION WITH ANISOTROPIC SCATTERING

Ser Gi Hong, Sang Ji Kim, Young Jin Kim, and Yeong Il Kim
Korea Atomic Energy Research Institute
Duckjin-dong, Yusong-gu, Taejon, Korea
hongsg@kaeri.re.kr; sjkim3@kaeri.re.kr; youkim@kaeri.re.kr; yikim1@kaeri.re.kr

ABSTRACT

A new high-order nodal method using the eigenfunction expansion and subcell balances for solving the slab-geometry discrete ordinates even-parity transport problems with anisotropic scattering is presented. The method uses five-term expansions including one constant term of the even-parity angular flux in a node. The expansion functions are the eigenfunctions of the transport equation. To derive the nodal coupling equations, the continuity conditions of the interface odd-parity angular flux and two subcell balances are used. For S_4 angular quadrature, the method gives the exact solution having no spatial truncation error because there are no approximations in this case. For higher order angular quadrature than S_4, the even-parity angular flux is expanded by four eigenfunctions corresponding to four large (in absolute value) eigenvalues or the eigenfunctions of the S_4 transport equation. For verification, the numerical results are compared with those of the diamond differencing (DD), the linear moment (LM) method, and the infinite medium Green's function (IMGF) method.

1. INTRODUCTION

In the past several decades, there have been significant advances [1,2] in nodal methods for solving the neutron diffusion problems. The methods use the expansion of the neutron flux or the transverse leakages by polynomials or analytic basis functions. These successes have led to some applications of these nodal methods to even-parity or simplified P_N equation [3,4]. For the second-order form or even-parity transport equation, most numerical methods use the finite difference method (FDM) and the finite element method (FEM) based on the variational formulation. For first-order form of the transport equation, there have been several efforts to develop highly accurate nodal methods [5,6,7,8]. These methods uses a set of eigenfunctions of the transport equation. The subcell balance methods that are a kind of the finite volume methods have been popularly used in nodal methods for solving the first-order form of the transport equations. Recently, the authors [9,10] have developed the function expansion nodal methods based on subcell balances [11,12,13] for solving the discrete ordinates even-parity transport equation in slab geometry. In this paper, the eigenfunction expansion methods (EEM) [10] are extended to anisotropic scattering problems. At present, we considered only linearly anisotropic scattering (the extensions for high-order anisotropic scattering are straightforward.). We show that the eigenfunction expansion nodal methods with anisotropic scattering can be formulated with slight modifications of the isotropic case because of the use of the similar eigenfunction expansion. The difference from the isotropic case is the relation between odd- and even-parity angular fluxes. Basically, our nodal methods use five expansion terms including one constant describing a particular solution. The interface continuity conditions of the odd-parity angular flux and two neutron balance conditions for two half subcells in a node are used to derive the nodal coupling equations. For S_4 angular quadrature set, the eigenfunction expansion method leads to an exact differencing scheme since there are no approximations. For angular quadrature sets higher than

S_4, we used two methods of expansion : in the first method, the eigenfunctions of the S_4 transport equation are used under the assumption that the spatial distribution of the solution weakly depends on the order of angular quadrature, and in the second method, four eigenfunctions corresponding to four large (in absolute value) eigenvalues are used. For verification, our method is applied to two benchmark problems. The numerical results are compared with those of the diamond differencing (DD), the linear moment (LM) method, and the infinite medium Green's function (IMGF) method.

2. THEORY AND COMPUTATIONAL METHOD

The derivation of our method starts with the following mono-energetic transport equation of second-order form with linearly anisotropic scattering in slab geometry :

$$-\mu_m \frac{\partial}{\partial x}\left(\frac{\mu_m}{\sigma}\frac{\partial \psi_m^+(x)}{\partial x}\right)+\sigma\psi_m^+(x)=\sigma_s\sum_{n=1}^{N/2} w_n\psi_m^+(x)-3\mu_m^2\frac{\partial}{\partial x}[c_1(x)J(x)]+q, \tag{1}$$

where w_n is the angular weight normalized by $\sum_{n=1}^{N} w_n = 2$, N is the order of angular quadrature, $\psi_m^+(x)$ represents the even-parity angular flux, and $J(x)=\sum_{n=1}^{N/2} w_n\mu_n\psi_n^-(x)$ is the net current. In Eq.(1), $c_1=\sigma_{s1}/\sigma$ is the scattering ratio of the linearly anisotropic scattering component. The odd-parity angular flux $\psi_m^-(x)$ is related with the even-parity angular flux through the following equation :

$$\psi_m^-(x)=-\frac{\mu_m}{\sigma}\frac{\partial\psi_m^+}{\partial x}+3c_1(x)\mu_m J(x). \tag{2}$$

In Eq.(2), it must be noted that its right hand side is also related with $\psi_m^-(x)$ through the net current while the net current term doesn't exist in the isotropic scattering case. It can be easily shown that Eq.(2) is a special case of the following general relation :

$$\begin{aligned}\psi_m^-(x)&=-\frac{\mu_m}{\sigma}\frac{\partial\psi_m^+}{\partial x}+\sum_{l=odd}(2l+1)c_{sl}(x)P_l(\mu_m)\phi_l(x),\\ \phi_{l=odd}(x)&=\sum_{n=1}^{N/2} w_n P_l(\mu_n)\psi_n^-(x),\end{aligned} \tag{3}$$

In our method, the even-parity angular flux in a node ($-h/2<x<+h/2$) is expanded as follows :

$$\psi_m^+(x)=a_m\sinh\left(\frac{\sigma x}{\nu_1}\right)+b_m\cosh\left(\frac{\sigma x}{\nu_1}\right)+c_m\sinh\left(\frac{\sigma x}{\nu_2}\right)+d_m\cosh\left(\frac{\sigma x}{\nu_2}\right)+\frac{q}{\sigma_a}. \tag{4}$$

Eq.(4) is devised from the fact that the general solution consists of a particular solution and the homogeneous solution. Therefore, it is desirable that the basis functions of Eq.(4) are the eigenfunctions of the homogeneous equation of Eq.(1). From a spectral analysis, it can be shown that the eigenfunctions are the exponential functions of $e^{-\sigma x/\nu}$ and the eigenvalues ν are determined by

$$\sum_{n=1}^{N/2} w_n\frac{c_0+3\mu_n^2c_1(1-c_0)}{1-\frac{\mu_n^2}{\nu^2}}=1, \tag{5}$$

where $c_0=\sigma_s/\sigma$. For S_N, N eigenvalues exist symmetrically around origin [5,7]. In this paper, the

hyperbolic functions rather than the exponential functions are used as the basis functions in Eq.(4) because the hyperbolic functions are even or odd and these characteristics make the derivations of the coupling equation easy. Therefore, we implemented two methods in the selection of eigenfunctions : first (EEM1) is the use of the S_4 eigenfunctions under the assumption that the spatial distribution of the solution weakly depends on the order of angular quadrature and second (EEM2) is to use four eigenfunctions corresponding to four large (in absolute value) eigenvalues of the S_N transport equation. The derivations for two methods are the same because two methods use the same expansion (i.e., Eq.(4)) except the eigenvalues. Since there are four expansion coefficients, the four nodal variables are required to be used. Following two even-parity interface angular fluxes ($\psi^+_{m,L}, \psi^+_{m,R}$) and two subcell average even-parity angular fluxes ($\psi^+_{m,hL}, \psi^+_{m,hR}$) are used as the nodal variables :

$$\begin{aligned}
\psi^+_{m,L} &= \psi^+_m(x=-h/2),\\
\psi^+_{m,R} &= \psi^+_m(x=+h/2),\\
\psi^+_{m,hL} &= \frac{2}{h}\int_{-h/2}^{0} dx\,\psi^+_m(x),\\
\psi^+_{m,hR} &= \frac{2}{h}\int_{0}^{+h/2} dx\,\psi^+_m(x)
\end{aligned} \tag{6}$$

By using Eq.(4) and the definitions of the nodal variables, the following relations between the nodal variables and the expansion coefficients can be derived :

$$\begin{aligned}
b_m &= \alpha(\psi^+_{m,L} + \psi^+_{m,R} - \frac{2q}{\sigma_a}) + \beta(\psi^+_{m,hL} + \psi^+_{m,hR} - \frac{2q}{\sigma_a}),\\
d_m &= \alpha_1(\psi^+_{m,L} + \psi^+_{m,R} - \frac{2q}{\sigma_a}) + \beta_1(\psi^+_{m,hL} + \psi^+_{m,hR} - \frac{2q}{\sigma_a}),\\
a_m &= \gamma(\psi^+_{m,R} - \psi^+_{m,L}) + \lambda(\psi^+_{m,hR} - \psi^+_{m,hL}),\\
b_m &= \gamma_1(\psi^+_{m,R} - \psi^+_{m,L}) + \lambda_1(\psi^+_{m,hR} - \psi^+_{m,hL}),
\end{aligned} \tag{7}$$

where $\alpha, \beta, \gamma, \lambda, \alpha_1, \beta_1, \gamma_1, \lambda_1$ are represented by $\cosh(\frac{\sigma h}{2\nu_i}), \sinh(\frac{\sigma h}{2\nu_i})$. For example, α and β are given by

$$\begin{aligned}
\alpha &= \frac{\frac{4\nu_2}{\sigma h}\sinh(\frac{\sigma h}{2\nu_2})}{\frac{8\nu_2}{\sigma h}\sinh(\frac{\sigma h}{2\nu_2})\cosh(\frac{\sigma h}{2\nu_1}) - \frac{8\nu_1}{\sigma h}\sinh(\frac{\sigma h}{2\nu_1})\cosh(\frac{\sigma h}{2\nu_2})},\\
\beta &= \frac{-2\cosh(\frac{\sigma h}{2\nu_2})}{\frac{8\nu_2}{\sigma h}\sinh(\frac{\sigma h}{2\nu_2})\cosh(\frac{\sigma h}{2\nu_1}) - \frac{8\nu_1}{\sigma h}\sinh(\frac{\sigma h}{2\nu_1})\cosh(\frac{\sigma h}{2\nu_2})}.
\end{aligned} \tag{8}$$

To derive the nodal coupling equation, the following subcell balance equations are obtained by integrating Eq.(1) over two halves of the node :

$$\mu_m(\psi^-_{m,C}-\psi^-_{m,L})+\sigma\psi^+_{m,hL}\frac{h}{2}=\sigma_s\phi_{hL}\frac{h}{2}+q_{hL}\frac{h}{2},$$
$$\mu_m(\psi^-_{m,R}-\psi^-_{m,C})+\sigma\psi^+_{m,hR}\frac{h}{2}=\sigma_s\phi_{hR}\frac{h}{2}+q_{hR}\frac{h}{2}, \tag{9}$$

where $\psi^-_{m,C}$ represents the odd-parity angular flux at the node center. By using Eq.(2), this equation can be written by

$$-\frac{\mu_m^2}{\sigma}\frac{\partial\psi^+_m}{\partial x}|_C+\frac{\mu_m^2}{\sigma}\frac{\partial\psi^+_m}{\partial x}|_L+\sigma\psi^+_{m,hL}\frac{h}{2}=\sigma_s\phi_{hL}\frac{h}{2}-3\mu_m^2[c_1J(x)]_C+3\mu_m^2[c_1J(x)]_L+q_{hL}\frac{h}{2},$$
$$-\frac{\mu_m^2}{\sigma}\frac{\partial\psi^+_m}{\partial x}|_R+\frac{\mu_m^2}{\sigma}\frac{\partial\psi^+_m}{\partial x}|_C+\sigma\psi^+_{m,hR}\frac{h}{2}=\sigma_s\phi_{hR}\frac{h}{2}-3\mu_m^2[c_1J(x)]_R+3\mu_m^2[c_1J(x)]_C+q_{hR}\frac{h}{2}. \tag{10}$$

After some algebra, the derivatives in Eq.(10) associated with the odd-parity angular fluxes can be represented in terms of the nodal variables through the same expressions as in the isotropic case (but with different eigenvalues). Substituting the representations into Eq.(10) gives the following equations :

$$G_{1m}\psi^+_{m,hR}+G_{2m}\psi^+_{m,hL}=G_{3m}\psi^+_{m,R}+G_{4m}\psi^+_{m,L}-3\mu_m^2[[c_1J]_C-[c_1J]_L]+\sigma_s\phi_{hL}\frac{h}{2}+q_{hL}\frac{h}{2},$$
$$G_{2m}\psi^+_{m,hR}+G_{1m}\psi^+_{m,hL}=G_{4m}\psi^+_{m,R}+G_{3m}\psi^+_{m,L}-3\mu_m^2[[c_1J]_R-[c_1J]_C]+\sigma_s\phi_{hR}\frac{h}{2}+q_{hR}\frac{h}{2}. \tag{11}$$

The next nodal coupling equation is obtained by using the continuity conditions of the interface odd-parity angular fluxes (i.e., $\psi^-_{m,R,i}=\psi^-_{m,L,i+1}$). The resulting equation is given by

$$(T_{1m,i}+T_{1m,i+1})\psi^+_{m,i+1}+T_{2m,i}\psi^+_{m,i}+T_{2m,i+1}\psi^+_{m,i+2}=T_{3m,i}\psi^+_{m,hR,i}+T_{4m,i}\psi^+_{m,hL,i}+T_{5m,i}\frac{2q_i}{\sigma_{a,i}}$$
$$+T_{4m,i+1}\psi^+_{m,hR,i+1}+T_{3m,i+1}\psi^+_{m,hL,i+1}+T_{5m,i+1}\frac{2q_{i+1}}{\sigma_{a,i+1}}+3\mu_m c_{1,i}J_{i+1}-3\mu_m c_{1,i+1}J_{i+1}, \tag{12}$$

where $\psi^+_{m,i+1}$ and J_{i+1} mean the even-parity angular flux and the net current, respectively, at the interface between node *i* and node *i+1*. In Eq.(12), the coefficients T are the same as those of the isotropic scattering (but with different eigenvalues). For simplicity, the only vacuum condition at the let boundary is described as follows :

$$\psi^+_m(0)-\frac{\mu_m}{\sigma}\frac{\partial\psi^+_m}{\partial x}|_{x=0}=0. \tag{13}$$

Representing the derivative in terms of the nodal variables and substituting it into Eq.(13) give

$$\psi^+_{m,1}+T_{2m,1}\psi^+_{m,2}+T_{1m,1}\psi^+_{m,1}-T_{4m,1}\psi^+_{m,hR,1}-T_{3m,1}\psi^+_{m,hL,1}-T_{5m,1}\frac{2q_1}{\sigma_{a,1}}=0. \tag{14}$$

To start the scattering source iteration, the subcell average scalar fluxes, the net currents, and the interface even-parity angular fluxes in Eq.(11) are initially assumed and then Eqs.(11) for all nodes are solved to give new subcell average even-parity angular fluxes. Next, Eqs.(12) representing the continuity of the odd-parity angular fluxes at all interfaces and the equations representing the boundary conditions are solved to obtain the updated interface even-parity angular fluxes.

3. NUMERICAL VERIFICATIONS

To verify the nodal methods, two benchmark problems are considered. The first problem consists of a homogeneous slab having $\sigma = 1.0$, $\sigma_s = 0.999$, $\sigma_{s1} = 0.2$ and thickness of 40.0cm. The vacuum condition is used at both the boundaries. The unit of all cross sections is cm^{-1}. A uniform isotropic inhomogeneous source having a strength of 10.0 n/cm^3sec is located in the region between 10.0 and 20.0cm from the left boundary. In Table I, the results are compared with the diamond difference (DD), the linear moment (LM) and the infinite Green function (IMGF) methods (no truncation error)[7,8]. All numerical results are obtained by using the S_4 angular quadrature set.

Table I. Percent errors in the region average scalar fluxes for benchmark problem I (S_4)

Region	Mesh Size (cm)	DD	LM	EEM	IMGF (Scalar flux)
1 (0<x<10)	10.000	5.438	2.151	0.000	625.4917
	5.000	1.169	0.244	0.000	
	2.500	0.286	0.005	0.000	
	1.250	0.073	-0.003	0.000	
	0.625	0.018	-0.001	0.000	
	0.313	0.004	0.000	0.000	
2 (10<x<20)	10.000	-9.043	-6.326	0.000	1446.411
	5.000	-2.261	-0.966	0.000	
	2.500	-0.562	-0.116	0.000	
	1.250	-0.140	-0.011	0.000	
	0.625	-0.035	-0.001	0.000	
	0.313	-0.009	0.000	0.000	
3 (20<x<30)	10.000	4.899	2.275	0.000	967.6820
	5.000	1.109	0.339	0.000	
	2.500	0.280	0.035	0.000	
	1.250	0.071	0.002	0.000	
	0.625	0.017	0.000	0.000	
	0.313	0.004	0.000	0.000	
4 (30<x<40)	10.000	4.446	1.422	0.000	328.2455
	5.000	1.078	0.114	0.000	
	2.500	0.257	-0.016	0.000	
	1.250	0.063	-0.006	0.000	
	0.625	0.015	-0.001	0.000	
	0.313	0.004	0.000	0.000	

As expected, the results show that the EEM method gives the exact value of the region average scalar fluxes irrespective of mesh size for the S_4 angular quadrature because there are no approximations in solving the discrete ordinates transport equation. That is to say, this method has no spatial truncation errors with the S_4 angular quadrature. This problem is also solved by using the S_8 angular quadrature to show how the accuracies of EEM1 and EEM2 change with the mesh size. For this angular quadrature, both EEM1 and EEM2 are not exact method. Figure. 1a and 1b show the percent errors of the region 2 and 4 average scalar fluxes over the mesh size, respectively. The percent errors of all region average scalar fluxes are compared in Table II. From Figure 1a and 1b, it is shown that EEM1 and EEM2 give highly accurate solutions irrespective of mesh size. For all mesh sizes, the percent errors are less than 0.3%. EEM1 gives more accurate solution than EEM2. Also, the results show that the errors of all methods in Table II decrease monotonically as the mesh size decreases.

Table II. Percent errors in the region average scalar fluxes for benchmark problem I (S_8)

Region	Mesh size (cm)	DD	LM	EEM1	EEM2	IMGF (Scalar flux)
1 (0<x<10)	10.000	5.378	2.107	0.093	0.228	626.9038
	5.000	1.215	0.235	0.085	0.173	
	2.500	0.284	-0.004	0.059	0.093	
	1.250	0.072	-0.009	0.023	0.030	
	0.625	0.018	-0.002	0.004	0.005	
	0.313	0.004	0.000	0.000	0.000	
2 (10<x<20)	10.000	-9.048	-6.229	0.025	0.070	1447.39
	5.000	-2.239	-0.936	0.025	0.054	
	2.500	-0.564	-0.110	0.018	0.029	
	1.250	-0.140	-0.012	0.007	0.010	
	0.625	-0.035	-0.001	0.001	0.002	
	0.313	-0.009	0.000	0.000	0.000	
3 (20<x<30)	10.000	4.895	2.213	0.033	0.072	968.42
	5.000	1.147	0.323	0.029	0.056	
	2.500	0.269	0.031	0.020	0.030	
	1.250	0.071	0.000	0.007	0.010	
	0.625	0.017	-0.001	0.001	0.001	
	0.313	0.004	0.000	-0.001	-0.001	
4 (30<x<40)	10.000	4.510	1.455	0.102	0.269	329.09
	5.000	1.194	0.119	0.098	0.202	
	2.500	0.259	-0.024	0.070	0.109	
	1.250	0.064	-0.012	0.027	0.036	
	0.625	0.016	-0.002	0.005	0.006	
	0.313	0.005	-0.000	0.000	0.000	

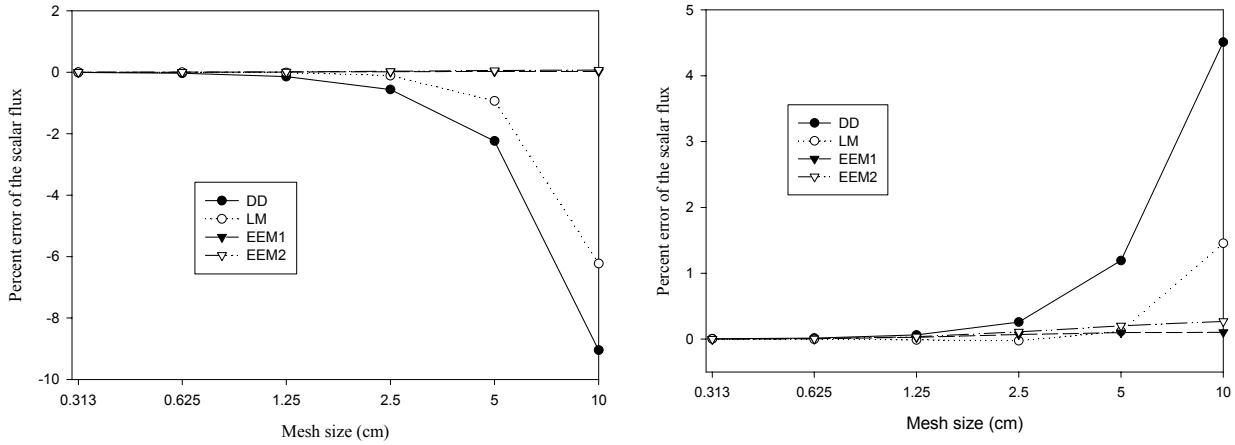

(a) Region 2 (b) Region 4

Figure 1. Percent errors of the region average scalar flux for benchmark problem I

The second problem consists of four different regions where the thickness of each region is 20.0cm. This problem is highly heterogeneous. The leftmost region (region 1) has $\sigma = 5.0$, $\sigma_s = 4.0$, $\sigma_{s1} = 0.45$ and $q = 10.0$. Next right region (region 2) has $\sigma = 2.0, \sigma_s = 0.7$, $\sigma_{s1} = 0.09$ and $q = 0.0$. Next right region (region 3) has $\sigma = 4.0, \sigma_s = 2.0$, $\sigma_{s1} = 0.4$ and $q = 5.0$. The rightmost region (region 4) has $\sigma = 1.0, \sigma_s = 0.99$, $\sigma_{s1} = 0.08$ and $q = 1.0$. The numerical results are obtained with the S_8 angular quadrature set. The results are shown in Figure 2 and Table III. The results show that EEM1 gives accurate solutions even when only one mesh per region is used. The percent error of EEM1 is less than 0.6%. On the other hand, EEM2 gives larger errors in region 2 where the absorption is highly dominant and the scalar flux is very low. The percent error of EEM2 for this region is nearly 4.0% when one mesh per region is used. The error decreases monotonically as the mesh size decreases. For other regions, EEM2 gives highly accurate solutions even when only one mesh per region is used. For this problem, it is noted that the solution of DD converges very rapidly to the exact solution although this problem is highly heterogeneous. However, it is observed that the negative fluxes occurred in the region 2 when the mesh size is larger than 0.5cm. Therefore, there seems no physical justification for the good accuracy of DD in the region 2.

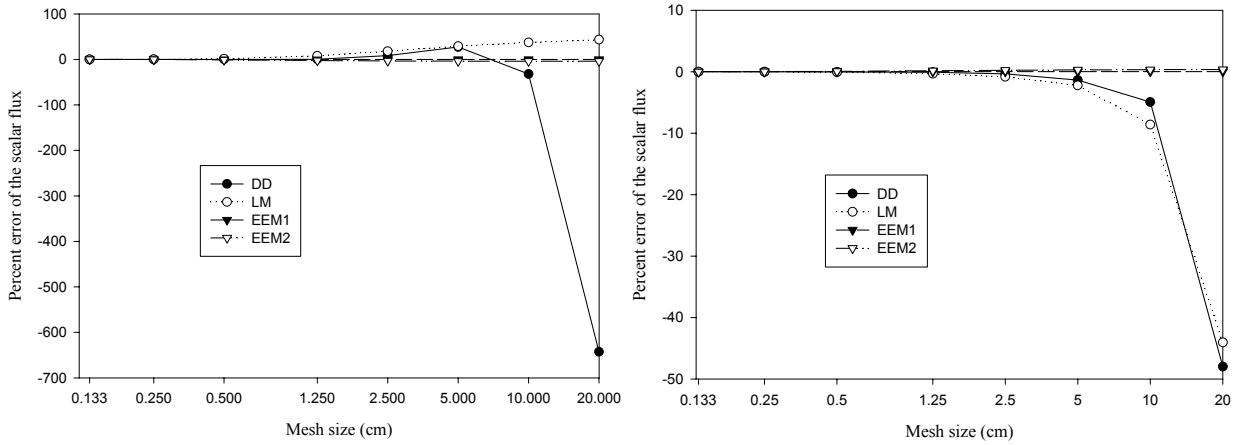

(a) Region 2 (b) Region 4

Figure 2. Percent errors of the region average scalar flux for benchmark problem II

Table III. Percent errors in the region average scalar fluxes for benchmark problem II (S_8)

Region	Mesh Size (cm)	DD	LM	EEM1	EEM2	IMGF (**Scalar flux**)
1 (0<x<20)	20.000	6.852	-0.828	0.005	0.044	9.8343
	10.000	1.612	-0.684	0.005	0.045	
	5.000	0.936	-0.539	0.005	0.044	
	2.500	0.102	-0.342	0.005	0.041	
	1.250	0.006	-0.151	0.008	0.033	
	0.500	0.000	-0.025	0.008	0.033	
	0.250	0.000	-0.004	0.003	0.015	
	0.133	0.000	-0.001	0.001	0.005	
2 (20<x<40)	20.000	-642.696[a]	43.486	-0.065	-3.818	0.081697
	10.000	-32.281[a]	37.195	-0.065	-3.818	
	5.000	27.186[a]	28.921	-0.072	-3.780	
	2.500	8.287[a]	18.014	-0.175	-3.435	
	1.250	0.328[a]	7.863	-0.476	-2.534	
	0.500	0.000[a]	1.322	-0.507	-1.049	
	0.250	0.000	0.231	-0.202	-0.306	
	0.133	0.000	0.035	-0.043	-0.060	
3 (40<x<60)	20.000	8.655	2.149	0.003	0.006	2.60549
	10.000	-3.290	0.385	0.002	0.007	
	5.000	-1.820	0.085	0.002	0.007	
	2.500	-0.266	0.028	0.002	0.006	
	1.250	-0.009	0.012	0.003	0.003	
	0.500	0.000	0.002	0.002	0.001	
	0.250	0.000	0.000	0.000	0.000	
	0.133	0.000	0.000	0.000	0.000	
4 (60<x<80)	20.000	-47.965	-44.037	0.028	0.360	51.2617
	10.000	-4.927	-8.590	0.035	0.339	
	5.000	-1.362	-2.233	0.039	0.300	
	2.500	-0.346	-0.812	0.031	0.241	
	1.250	-0.076	-0.330	0.015	0.168	
	0.500	-0.012	-0.058	0.018	0.061	
	0.250	-0.003	-0.010	0.008	0.016	
	0.133	-0.001	-0.001	0.001	0.002	

4. SUMMARY AND CONCLUSIONS

In this paper, a new nodal method for solving the discrete ordinates even-parity transport equation in slab geometry is presented. The nodal method uses the expansion of the even-parity angular flux in a node by using the eigenfunctions that satisfy the homogeneous transport equations. The number of

expansion terms including one constant is five. The nodal coupling equations are derived by using the continuity conditions of the interface odd-parity angular fluxes and two subcell balances for two half subcells. For higher angular quadrature than S_4, the angular flux is expanded by the eigenfunctions of the S_4 transport equation or four eigenfunctions corresponding to four large (in absolute value) eigenvalues and one constant term corresponding to a particular solution. The numerical results show that the nodal methods are very promising in that the solutions is very accurate even when only one mesh per region is used. In particular, it is shown that the expansion of the even-parity angular flux by using the eigenfunctions of the S_4 transport gives highly accurate solutions irrespective of mesh size. In the future, we are planning to extend this nodal method to two-dimensional problems and develop or implement an acceleration method for the scattering source iteration.

ACKNOWLEDGEMENTS

This work was supported by Nuclear R&D Long-Term Development Program of the Ministry of Science and Technology of Korea.

REFERENCES

1. R.D. Lawrence, "Progress in Nodal Methods for the Solution of the Neutron Diffusion and Transport Equations," *Prog. Nucl. Energ*., **17**, 271 (1986)
2. J. M. Noh and N. Z. Cho, "A New Approach of Analytic Basis Function Expansion to Neutron Diffusion Nodal Calculation," *Nucl. Sci. Eng*., **116**, 165 (1994).
3. J. Y. Cho, C. H. Kim and T. Noh, "Polynomial Expansion Nodal Transport Method in Hexagonal Geometry," *Trans. Am. Nucl. Soc*., **77**, 187 (1997).
4. T. Noh, "Development of the Discrete-Ordinates, Nodal Transport Methods Using the Simplified Even-Parity Neutron Transport Equation," *J. of Kor. Nucl. Soc*., **32**, No. 6, 605 (2000).
5. R. C. De Barros and E. W. Larsen, "A Numerical Method for One-Group Slab-Geometry Discrete Ordinates Problems with No Spatial Truncation Error," *Nucl. Sci. Eng*., **104**, 199 (1990).
6. R. C. De Barros, F. C. da Silva, and H. A. Filho, "Recent Advances in Spectral Nodal Methods for X,Y-Geometry Discrete Ordinates Deep Penetration and Eigenvalue Problems," *Prog. in Nucl. Energy*, **35** (3-4), 298 (1999).
7. S. G. Hong and N. Z. Cho, "An Analytic Solution Method for Discrete Ordinates Transport Equations in Slab Geometry with No Truncation Error," *Trans. Am. Nucl. Soc*., **81**, 134 (1999).
8. S. G. Hong and N. Z. Cho, "The Infinite Medium Green's Function Method for Multigroup Discrete Ordinates Transport Problems in Multi-Layered Slab Geometry," *Ann. of Nucl. Energy*., **28**, 1101 (2001).
9. S. G. Hong and Y. I. Kim, "A High-Order Nodal Method Based on the Function Expansion, Subcell Balances for Even-Parity Transport Problems," *Proc. of Korean Nuclear Society Autumn Meeting*, 2001, Suwon, Korea.
10. S. G. Hong et al., "High-Order Function Expansion Nodal Methods for the Even-Parity Transport Equation," *Submitted to the 2002 ANS Annual Meeting*, Hollywood, USA.
11. J. E. Morel and E. W. Larsen, "A Multiple Balance Approach for Differencing the S_N Equations," *Nucl. Sci. Eng*., **105**, 1 (1990).
12. C. L. Castrianni and M. L. Adams, "A Nonlinear Corner-Balance Spatial Discretization for Transport on Arbitrary Grids," *Nucl. Sci. Eng*., **128**, 278 (1998).
13. C. J. Park and N. Z. Cho, "A Linear Multiple Balance Method with High Order Accuracy for Discrete Ordinates Neutron Transport Equations," *Ann. of Nucl. Energy*, **28**, 1499 (2001).